Propensity of undulatory swimmers, such as worms, to go against the flow

Jinzhou Yuan[a], David M. Raizen[b], and Haim H. Bau[a,1]

[a]Department of Mechanical Engineering and Applied Mechanics and [b]Department of Neurology, Perelman School of Medicine, University of Pennsylvania, Philadelphia, PA 19104

Edited by David A. Weitz, Harvard University, Cambridge, MA, and approved February 10, 2015 (received for review December 30, 2014)

The ability to orient oneself in response to environmental cues is crucial to the survival and function of diverse organisms. One such orientation behavior is the alignment of aquatic organisms with (negative rheotaxis) or against (positive rheotaxis) fluid current. The questions of whether low-Reynolds-number, undulatory swimmers, such as worms, rheotax and whether rheotaxis is a deliberate or an involuntary response to mechanical forces have been the subject of conflicting reports. To address these questions, we use *Caenorhabditis elegans* as a model undulatory swimmer and examine, in experiment and theory, the orientation of *C. elegans* in the presence of flow. We find that when close to a stationary surface the animal aligns itself against the direction of the flow. We elucidate for the first time to our knowledge the mechanisms of rheotaxis in worms and show that rheotaxis can be explained solely by mechanical forces and does not require sensory input or deliberate action. The interaction between the flow field induced by the swimmer and a nearby surface causes the swimmer to tilt toward the surface and the velocity gradient associated with the flow rotates the animal to face upstream. Fluid mechanical computer simulations faithfully mimic the behavior observed in experiments, supporting the notion that rheotaxis behavior can be fully explained by hydrodynamics. Our study highlights the important role of hydrodynamics in the behavior of small undulating swimmers and may assist in developing control strategies to affect the animals' life cycles.

rheotaxis | hydrodynamics | *C. elegans* | nematode | microfluidics

Small organisms that swim with undulating anterior-to-posterior waves (undulatory microswimmers), such as round worms, are ubiquitous in nature. They play important roles in diverse ecosystems, including soils, fresh water, marine water, and, in the case of parasitic nematodes, mammalian intestinal tracts and bloodstreams and plants (1, 2). Parasitic nematodes cause human morbidity as well as livestock and plant diseases that result in severe economic damage, estimated in many billions of dollars annually (1–4). The nonparasitic, free-living nematode *Caenorhabditis elagans* is used as an animal model to study mechanisms that govern physiology and development.

In their habitats, nematodes are exposed to various environmental stimuli. The ability to adjust their direction of motion in response to diverse environmental cues plays an important role in the animals' life cycles. Understanding the mechanisms responsible for the animals' response to various cues is scientifically interesting (5) and useful for devising control strategies to alter the nematodes' life cycles and for the design of microfluidic systems. In this paper, we focus on rheotaxis, defined as the animal's orientation in response to fluid flow (6). Positive rheotaxis, in which the animals turn to face into an oncoming current, has been observed in a few aquatic organisms including the bacterium *Mycoplasma mobile* (7) and zebrafish larvae (8). Reports on rheotaxis in undulatory microswimmers are, however, conflicting. A few researchers claim that undulatory swimming nematodes do not exhibit rheotactic behavior (9–11), whereas others have reported evidence of rheotaxis in various nematodes, including the rice eater *Aphelenchoides besseyi* (12), the potato eaters *Meloidogyne chitwoodi* and *Meloidogyne hapla* (13), the root eater *Meloidogyne incognita* (14, 15), the banana eater *Radopholus similis* (16), the bacteria-eating *C. elegans* (17, 18), and the human parasites *Ancylostoma duodenale* and *Strongyloides stercoralis* (19). On occasion, rheotaxis can overcome other stimuli such as chemotaxis (13, 17). The mechanisms responsible for rheotaxis in undulatory swimmers have not yet been elucidated. In this paper, we examine the circumstances under which rheotaxis occurs and propose a hydrodynamic mechanism to explain this behavior.

We use the nematode *C. elegans* as a model of an undulatory swimmer and study both experimentally and theoretically its behavior in the presence of imposed flow. The first part of the paper describes our experimental results on the behavior of the animals in conduits of various widths and clarifies the conditions needed for rheotaxis. The experimental observations suggest that rheotaxis can be caused by hydrodynamic forces alone and does not require involvement of the animal's sensory systems. The second part of the paper focuses on fluid dynamics computer simulations that approximate our experimental conditions. The simulation results agree qualitatively with our experimental observations. We find both in experiment and theory that *C. elegans* exhibit robust, positive rheotaxis when they are close to a surface and that the rheotaxis in undulatory swimmers can be fully explained by the laws of mechanics.

Experiments

First, we monitored the direction of swimming of wild-type, adult *C. elegans* in a 100-μm-deep × 2.6-mm-wide conduit in the presence of water flow (300 μL/h) with average velocity of 321 μm/s that is comparable to the swimming speed of young adult *C. elegans* (Movie S1). The conduit is sufficiently tall and wide to accommodate uninhibited swimming but shallow enough to

Significance

Undulating swimmers, such as worms, are ubiquitous and play important roles in the ecosystem; agriculture; human, animal, and plant health; and medical research. The ability of undulatory swimmers to align against the flow (rheotax) is important in the animals' life cycles, enabling them to navigate their environment and to maintain their positions in the presence of adverse flows such as in the hosts' guts and blood vessels. We elucidate, for the first time to our knowledge, the mechanism responsible for rheotaxis in low-Reynolds-number, undulatory swimmers. This knowledge will provide a better understanding of the animals' life cycles, will enable the development of strategies to disturb their life cycles, and will improve the design of microfluidic devices for biological research.

Author contributions: J.Y. and H.H.B. designed research; J.Y. performed research; J.Y., D.M.R., and H.H.B. analyzed data; and J.Y., D.M.R., and H.H.B. wrote the paper.

The authors declare no conflict of interest.

This article is a PNAS Direct Submission.

[1]To whom correspondence should be addressed. Email: bau@seas.upenn.edu.

This article contains supporting information online at www.pnas.org/lookup/suppl/doi:10.1073/pnas.1424962112/-/DCSupplemental.

www.pnas.org/cgi/doi/10.1073/pnas.1424962112

keep the animals in the focal plane of the microscope and prevent them from rotating in the vertical plane. The majority of the animals swam upstream with their heads pointing into the flow, a behavior known as positive rheotaxis. We noted (Movie S1) that the animals aggregate next to the conduit's boundaries, exhibiting surface attraction (bordertaxis) (20), as well as occasional synchronized swimming when they are closely packed (21).

The experiment shown in Movie S1 raised a concern about a possible bias in favor of upstream swimmers, because downstream swimmers may have been washed out of the observation region and, therefore, were not counted. To address this concern, we increased the flow to a sufficiently high rate (3,000 μL/h) to carry all of the swimmers with the flow, regardless of their direction of swimming, and monitored the orientation of the animals as they passed through the conduit's cross-section located 1 cm downstream of the conduit's entrance. The corresponding average flow velocity 3,210 μm/s is about 10 times the typical swimming speed of young adult *C. elegans*. In this experimental configuration, all of the animals were counted, regardless of their orientation relative to the direction of flow. We designate the nematode's orientation with the angle θ formed between the line that connects the nematode's tail and head and the conduit's axis directed against the flow (Fig. 1*A*, *Inset*). We define the swimming direction as against the flow when $-90° < \theta < 90°$, and as with the flow when $90° < \theta < 270°$. In a conduit of width $W = 2.6$ mm, the majority of the animals (~73%) were oriented against the flow (Fig. 1*A*), suggesting that *C. elegans* does, indeed, exhibit a tendency to swim against the flow.

Our initial observations suggested that animals closer to the conduit boundary were more likely to be oriented against the flow. To further explore this observation we examined the orientation of the animals as a function of their transverse position in the conduit. Fig. 1*B* depicts the fraction of animals located at normalized transverse position $\bar{d} = 0.5 - |y/W|$ and oriented at $|\theta| \pm \Delta\theta/2$, where y is the distance of the animal's center of mass from the conduit's mid width ($0 < \bar{d} \leq 0.5$) and $\Delta\theta = 9°$. In support of our initial observations, Fig. 1*B* illustrates that the tendency of animals to orient against the flow is most pronounced in the vicinity of the conduit's boundary ($\bar{d} = 0$) and diminishes as the distance from the boundary increases. This analysis suggested that the side wall plays an important role in orienting the animals. However, what are the mechanisms involved?

To gain a deeper insight we examined closely the alignment process of individual animals in the presence of flow. Fig. 1*C* is composed of superposed video frames taken 0.125 s apart in the presence of an external fluid flow with average flow velocity of 3,210 μm/s (3,000 μL/h) directed from right to left. The frame sequence also proceeds from right to left. The position of the animal's head is indicated with a vertical, color-coded arrow. Blue arrows denote early times and red arrows later times. At time $t = 0$, the animal swims with the flow with a slight inclination toward the surface. Because the fluid velocity at the surface is zero and increases away from the surface (Fig. S1), the animal's tail is exposed to a higher fluid velocity than its head. Consequently, the animal's tail moves to the left (with the flow) faster than its head. After about 1.5 s, the animal has completed a nearly 180° turn, ending up aligned against the flow, and remains so (Movie S2). Fig. 1*D* (blue triangles) depicts the orientation angle θ as a function of time; $\theta(t = 0 \text{ s}) \sim 152°$ and $\theta(t = 1.5 \text{ s}) \sim 3°$.

Recently, we identified that low-Reynolds-number undulatory swimmers are attracted to surfaces (bordertaxis) (20). The interaction between the flow field induced by the swimmer's motion and the nearby surface generates a torque that tilts the swimmer toward the surface. This is a hydrodynamic effect that requires no involvement of the animal's nervous system. Touch-sensitive (wild-type) nematodes and touch-insensitive mutants were equally affected, indicating that the animal's mechanosensory system does not play a role in surface attraction. As a result of boundary attraction, animals that are close to the surface

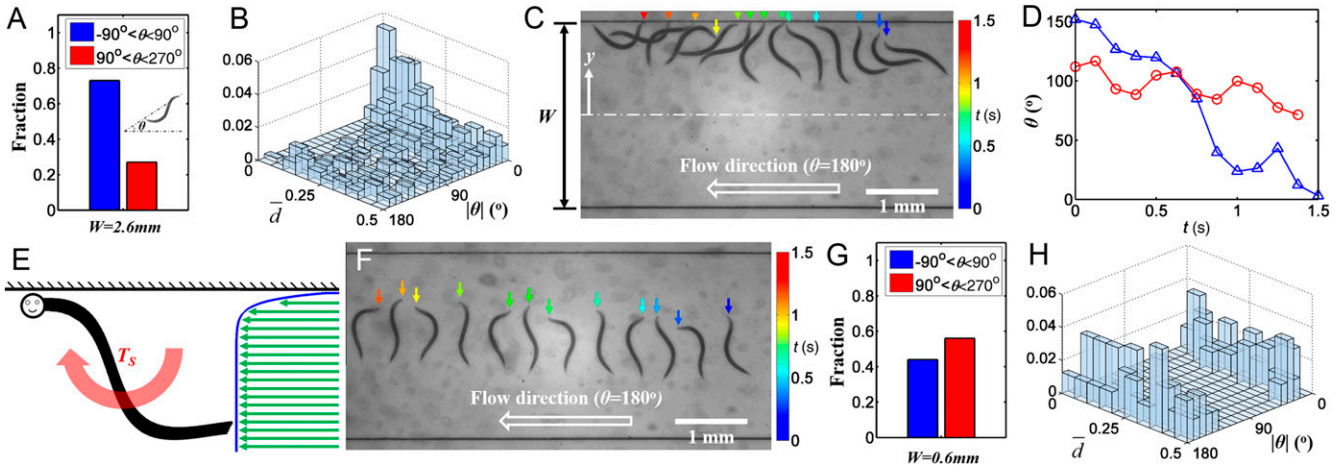

Fig. 1. (*A*) The fractions of animals in a 2.6-mm-wide conduit oriented against (blue bar, $-90° < \theta < 90°$) and with (red bar, $90° < \theta < 270°$) a flow in the $\theta = 180°$ direction. $n = 413$ animals. The observed distribution of animals into the two orientation groups was significantly different from the null distribution consisting of 50% of the animals in each group, $P < 0.0001$. (*B*) The fraction of the animals in a 2.6-mm-wide conduit (in the presence of flow in the $\theta = 180°$ direction) as a function of normalized distance from the closest surface ($\bar{d}$) and body orientation ($|\theta|$). $n = 413$ animals. (*C*) Superimposed images documenting the change in the orientation of an individual animal that was initially oriented with the flow next to the surface of a 2.6-mm-wide conduit as the animal is washed with the flow. The vertical arrows indicate the position of the animal's head and the colors indicate the time. See time scale to the right. (*D*) The angle formed between the swimmer and the conduit's axis (θ) as a function of time when the swimmer is close to the boundary (blue triangles, *C*) and away from the boundary (red circles, *F*). (*E*) A cartoon depicting conduit-depth averaged axial velocity as a function of distance from the conduit boundary (green arrows) and the torque applied to the swimmer by the external flow when the swimmer is inclined in the direction of flow. (*F*) Same as *C* except the animal is in the conduit's interior far from the surface. (*G*) The fractions of animals oriented against (blue bar, $-90° < \theta < 90°$) and with (red bar, $90° < \theta < 270°$) the flow in a 0.6-mm-wide conduit in the presence of fluid flow in the $\theta = 180°$ direction. The observed distribution of animals into the two orientation groups was not significantly different from the null distribution consisting of 50% of the animals in each group, $P = 0.37$. $n = 79$ animals. (*H*) The fraction of the animals in the 0.6-mm-wide conduit (in the presence of flow in the $\theta = 180°$ direction) as a function of normalized distance from the closest surface ($\bar{d}$) and body orientation ($|\theta|$).

swim toward the surface. In the presence of external flow there is a velocity gradient next to the surface, with zero velocity at the surface. In Fig. 1*E*, the arrows depict the velocity field averaged across the conduit's depth. The fluid velocity increases as the distance from the boundary increases. When the animal swims toward the surface, it would be inclined with respect to the direction of the flow with its tail (located further from the surface) being exposed to a higher velocity than its head (located closer to the surface). As a result, the external flow rotates the animal to align it against the flow. This alignment mechanism is purely hydrodynamic and does not require deliberate action by the animal. To reiterate, our experiments suggest that two factors are needed to align the swimmers against the flow. First, the swimmer must tilt toward the surface so that its head is closer to the surface than its tail. Second, a velocity gradient must be present to expose the swimmer's tail to higher velocity than its head and rotate the swimmer to face the flow. The presence of the surface provides both the tilting action and the velocity gradient. The interaction between the flow field induced by the swimmer and the surface causes the animal to tilt toward the surface both in the absence and presence of flow. The velocity gradient is due to the fact that the liquid velocity vanishes at the stationary surface.

If the above hypothesis is true, an immediate corollary would be that in the absence of velocity gradients in the plane of motion, animals would not align against the flow. Fig. 1*B* suggests that this is, indeed, the case. As the distance from the surface increases the velocity gradient along the conduit's width diminishes and the tendency to align against the flow decreases. To better understand the interaction of the animal with the flow in the absence of velocity gradients, we tracked in Fig. 1*F* an animal located close to the conduit's center (Movie S3), where the velocity profile along the conduit's width is nearly flat (Fig. S1). The figure is composed of superimposed video frames arranged from right to left. The color-coded, vertical arrows indicate the positions of the animal's head at various times with dark blue (on the right) corresponding to time $t = 0$ and light red (on the left) to $t = 1.375$ s. Witness that the animal's orientation remains nearly unaltered during this period. Fig. 1*D* (red circles) depicts the animal's orientation as a function of time and shows little change in the orientation during the course of the experiment. This, of course, is bound to change once the animal approaches the boundary and is subjected to a velocity gradient. The experiment documented in Fig. 1*F* indicates that in the presence of a uniform flow (in the absence of velocity gradients) the animals do not rheotax. Interestingly, when experimenting with hookworm larvae suspended in a glass box, Lane (9) did not observe rheotaxis in the presence of flow (presumably, the animals were far from surfaces). In contrast, he reported positive rheotaxis when the worms were in a capillary tube (presumably, proximate to a surface).

Our observations suggest that the mechanism of the animals' alignment against the flow is caused solely by hydrodynamic effects and does not require determined action on the animals' part. In other forms of orientation behavior (e.g., chemotaxis) *C. elegans* worms are known to make deliberate 180° turns by bending their body into the shape of the Greek letter omega. These so-called "omega" turns indicate deliberate behavior (22). To examine whether the animal's deliberate action is involved in rheotaxis we repeated the experiment of Fig. 1*B* with a narrower conduit ($W =$ 0.6 mm) at a flow rate of 460 μL/h and average velocity of 2,130 μm/s (about seven times the swimming speed of young adult *C. elegans)*. The conduit was too narrow to allow the 1- to 1.2-mm-long animals to change orientation by hydrodynamic effects (Movie S4) but was wide enough to allow them to make determined omega turns (Movie S5). Fig. 1*G* ($W = 0.6$ mm) shows that about half (56%) of the animals ($n = 79$) were oriented with the flow. Fig. 1*H* depicts the fraction of animals with their center of mass at a transverse position $\overline{d} \pm \Delta\overline{d}$ and oriented in the $|\theta| \pm \Delta\theta$ direction. The orientations of the animals were nearly independent of transverse positions, and about the same fraction of animals were oriented with the flow as against the flow. Hence, when a change of orientation by hydrodynamics is precluded, rheotaxis does not occur. This experiment provides further support to the notion that rheotaxis is caused by hydrodynamics and is not a deliberate action of the nematode.

Theoretical Calculations

If rheotaxis is caused solely by hydrodynamic effects, we should be able to reproduce a similar phenomenon in computer simulations that account only for passive mechanical forces. Because 3D simulations are time-consuming and the essence of the rheotaxis can be captured with 2D models, we solve the 2D Stokes equations for an undulatory swimmer in a conduit in the presence of flow. The simulation differs from the experiment in the absence of the conduit's floor and ceiling. The vertical confinement in the experiment increases the drag force acting on the swimmer (23) and screens the wall shear stress to reduce the extent of the velocity gradient next to the side walls. The 2D model does include, however, the key features responsible for rheotaxis such as the interaction between the flow field induced by the swimmer and the side wall and the presence of a velocity gradient. The detailed description of the mathematical model and the validation of the numerical code (Figs. S2 and S3) are presented in *Supporting Information*. Briefly, we approximate the *C. elegans* as a sinusoidal, undulating object with a uniform width. The animal's size and gait are selected to approximate an adult *C. elegans* (21). The swimmer's projected length along its direction of motion is 1,005 μm, its body width is 69 μm, its wavelength is 1,005 μm, its amplitude is 112.5 μm, and its frequency of bends is 1.7 Hz. The conduit's width is 2,600 μm. The liquid is water.

Because the swimmer's velocity and rotational speed are not a priori known, we superpose solutions of auxiliary problems, composed of a swimmer with a unit velocity in the x direction, a swimmer with a unit velocity in the y direction, a swimmer with a unit rotational velocity, and a stationary swimmer with a surface velocity distribution consistent with the nematode's undulatory gait. In the first three auxiliary problems we specify zero velocity at the conduit's inlet. In the last auxiliary problem we specify a parabolic profile at the inlet with an average velocity of 300 μm/s. In all cases we specify zero viscous stress at the conduit's outlet and nonslip conditions at all solid surfaces. Both the conduit's inlet and outlet are located more than five wavelengths away from the swimmer to minimize end effects on the calculations. The instantaneous x-direction velocity U, the y-direction velocity V, and the rotational velocity ω are obtained by requiring that no net forces and torque act on the swimmer. To account for the repulsive forces resulting from the collisions between the swimmer and the surface, the force balance equations are augmented with short-range Lennard-Jones–like repulsive terms:

$$\begin{pmatrix} 0 \\ 0 \\ 0 \end{pmatrix} = M(t) \begin{pmatrix} U(t) \\ V(t) \\ \omega(t) \end{pmatrix} + \begin{pmatrix} F_{U,x}(t) \\ F_{U,y}(t) \\ T_U(t) \end{pmatrix} + \begin{pmatrix} F_{S,x}(t) \\ F_{S,y}(t) \\ T_S(t) \end{pmatrix} + \begin{pmatrix} F_{C,x}(t) \\ F_{C,y}(t) \\ T_C(t) \end{pmatrix}. \quad [1]$$

In the above, M is the time-dependent numerically computed 3×3 resistance matrix, F_x and F_y are, respectively, the x and y components of the force, and T is the torque. The subscripts U, S, and C denote, respectively, the contributions of the undulatory motion, background flow, and steric Lennard-Jones–like hindrance. We compute $M(t)$, $F_{U,x}(t)$, $F_{U,y}(t)$, $F_{S,x}(t)$, $F_{S,y}(t)$, $T_U(t)$, and $T_S(t)$ with the finite element program COMSOL. The

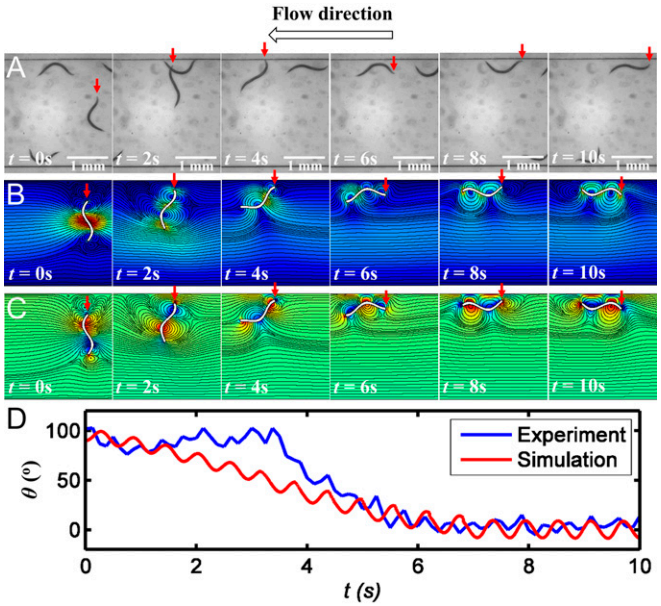

Fig. 2. Comparison of the (*A*) experimentally observed and (*B* and *C*) computer-simulated change of orientation of an undulatory swimmer near a surface in the presence of fluid flow directed to the left ($\theta = 180°$). Red arrows denote the position of the animal's head. (*D*) The animal's measured (blue) and predicted (red) orientation (θ) as a function of time. Color in *B* and *C* depicts, respectively, the velocity field and the vortex field. The solid lines in both *B* and *C* are stream lines.

trajectory of the swimmer is obtained by integrating the kinetic equations in time:

$$\begin{pmatrix} \dot{X}(t) \\ \dot{Y}(t) \\ \dot{\theta}(t) \end{pmatrix} = \begin{pmatrix} U(t) \\ V(t) \\ \omega(t) \end{pmatrix}. \qquad [2]$$

Fig. 2*A* depicts from left to right video frames of an experimental recording of a swimmer. Initially ($t = 0$), the swimmer's center of mass is distance $y(0) = 300$ μm from the conduit's mid width and the swimmer is nearly perpendicular to the flow direction [$\theta(0) \sim 90°$]. The head of the swimmer of interest is identified with a red, vertical arrow. The flow is from right to left, and the frames are spaced 2 s apart. As time goes by, the swimmer approaches the boundary and rotates to orient itself against the flow. Fig. 2 *B* and *C* depict the computed position and orientation of the theoretical swimmer with initial conditions similar to the ones in the experiment. Fig. 2*B* depicts the instantaneous velocity field and stream lines (solid lines). Fig. 2*C* depicts the instantaneous vorticity field and stream lines (solid lines). The predicted counterrotating vortex pair agrees well with available flow visualization experiments (24, 25). As the swimmer approaches the side wall, its head enters a region of low velocity while its tail remains exposed to a higher velocity ($t = 2$ s). As a result, the external flow rotates the swimmer to face into the flow ($t = 6$ s). Once it is swimming next to the wall and against the flow, the interaction between the flow field induced by the swimmer's gait and the wall tilts the swimmer toward the wall ($t = 8$ s), reducing the probability of the animal's departing from the wall region. The computer-simulated trajectories of the animal are in qualitative agreement with experimental observations. Movie S6 provides a vivid comparison of the computer animations and experimental observations. The similarity in behavior is striking. Fig. 2*D* depicts the experimentally observed (blue) and the predicted (red) instantaneous inclination angle θ as functions of time. The striking resemblance between the theoretical predictions and experimental observations reinforces the notion that the change in the swimmer's orientation to align itself against the flow is caused by hydrodynamic effects.

Next, we examine the fraction of animals with their center of mass initially at $y(0) = -300$ μm that end up aligned against the flow as a function of their initial orientation $\theta(0)$. To this end, we simulate the motion of animals with various initial inclination angles subject to the same flow conditions as in Fig. 2. Fig. 3*A* depicts the trajectories of animals with $\theta(0) = -145°$-ε, $-145°$+ε, 155°-ε, and 155°+ε, where ε = 5°. Fig. 3*B* depicts the instantaneous angles $\theta(t)$ as functions of time for the four above cases. In all instances the animal initially has a velocity component in the direction of the external flow, eventually arrives close to the surface, and ends up swimming along the surface either with (red trajectories) or against (blue trajectories) the flow. The region shaded in blue in Fig. 3*A* ($-145° \leq \theta(0) \leq 155°$) identifies the initial conditions that resulted in the animal's eventually facing upstream. If the initial orientation of the swimmer were a uniformly distributed random variable and only hydrodynamic factors were at play, the simulations predict that ~83% of the swimmers originating at $y(0) = -300$ μm will end up with upstream orientation, which is on par with the experimental data (73%) of Fig. 1*A*. The calculations of Fig. 3*A* were repeated for animals having the initial positions of their centers of mass at $0 > \bar{y}(0) > -0.15$ and the results are summarized in Fig. 3*C*. The blue and red regions in Fig. 3*C* identify, respectively, the initial conditions that eventually lead to upstream and downstream swimming.

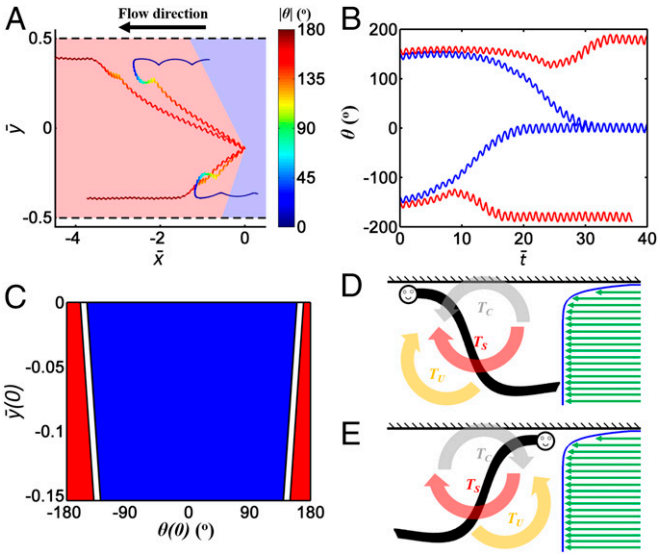

Fig. 3. (*A*) Four computed trajectories of animals' centers of mass for animals initially located at $\hat{y} = y/W = -0.12$ and oriented at $\theta(0) = -150°$, $-140°$, 150, and 160°. The lengths are scaled with the conduit's width $W = 2.6$ mm. The external flow is directed to the left ($\theta = 180°$). The trajectory's color indicates the angle θ. See scale on the right. The regions shaded in blue and pink identify, respectively, the initial conditions that result in the animal eventually facing upstream and downstream. (*B*) The orientation angles θ of the four animals whose trajectories were depicted in *A* as functions of time normalized with the swimming period. Blue and red denote, respectively, animals whose final orientation was against and with the flow. (*C*) The eventual orientation of the animal (blue and red correspond to against and with the flow respectively) as a function of the initial position of the animal's center of mass $\bar{y}(0)$ and orientation $\theta(0)$. (*D* and *E*) Schematic depiction of the various torques experienced by downstream and upstream swimmers. T_C denotes torque produced by collisions of the animal's head with the boundary, T_S denotes torque produced by the differences in velocity at the location of the tail and the head of an inclined animal, and T_U denotes torque associated with the flow field induced by an undulating animal to orient it toward the surface (bordertaxis).

To gain further insight on the behavior of nematodes close to surfaces we examine in Fig. 3 *D* and *E* the various torques that act on downstream and upstream swimmers. In prior work (20) we have shown that in the absence of external flow, the flow field induced by the undulatory swimmer interacts with the surface to induce torque T_U that tilts the swimmer toward the surface, placing it on a collision course with the surface. Once the animal collides with the surface, its center of mass is repelled from the surface to allow it to maintain its far field gait. We denote the torque resulting from this collision T_C. Once repelled from the surface, the hydrodynamic torque T_U restores the animal's direction of motion back toward the surface. This interplay between short-range attractive hydrodynamic force and repulse steric force enables the animal to swim along the surface for extended time intervals. In the presence of external flow, when the animal is inclined toward the surface, the animal's tail is exposed to a higher external velocity than its head, subjecting the animal to the torque T_S induced by the external flow. When the animal swims with the flow, T_S rotates the animal to orient it against the flow, destabilizing the downstream swimming state (Fig. 3*D*). When the animal swims against the flow, T_S stabilizes the upstream swimming state (Fig. 3*E*). As a result, most animals, regardless of their initial orientation and position, will eventually end up swimming upstream.

Would the majority of the animals align against the flow solely by a geometric effect in the absence of boundary attraction? Assuming that the orientation of animals located away from the wall is uniformly distributed, most of the animals that are not already oriented against the flow will eventually reach one of the side walls. When the animal approaches a side wall, its head will be closer to the wall than its tail. As a result, the torque T_S will orient the animal to face into the flow. In the absence of surface attraction, the animals are unlikely to stay in the wall's vicinity. Once the animals head away from the wall, the torque T_S will align them with the flow. Thus, it is unlikely that the conduit geometry alone would cause the majority of animals to align against the flow.

Conclusions

We examined both experimentally and theoretically the effect of fluid flow on the orientation of undulatory swimmers using the nematode *C. elegans* as a model animal. We found that in the presence of a velocity gradient next to stationary surface, most undulatory swimmers align themselves against the direction of the flow (positive rheotaxis) with their heads facing upstream. In contrast to other tactic behaviors, such as chemotaxis (26), thermotaxis (27), and electrotaxis (28), which require active involvement of the nervous system, rheotaxis results from purely mechanical interactions.

Assuming that animals located far from the conduit's side walls are randomly oriented, most swimmers eventually arrive at the side walls. In the presence of externally imposed flow, there will be a velocity gradient next to the wall that rotates animals swimming toward the wall to face into the flow. If the animal were to bounce back and head away from the wall, the velocity gradient next to the surface will rotate the animal to orient it with the flow and likely no preferred orientation would be observed. For the majority of animals to be oriented against the flow we need yet additional mechanism to retain the animals in the wall vicinity. Once next to the conduit's side wall, the interaction between the undulatory swimmer-induced flow field and the wall rotates the swimmer toward the wall (boundary attraction), causing the swimmer's anterior to collide with the surface (20). Once the swimmer rebounds, surface attraction restores the rotation toward the wall. The interplay between hydrodynamic attraction to the surface and steric repulsion enables the animal to swim along the surface for extended time intervals. In the presence of the external flow, the velocity gradient induces a torque that stabilizes upstream swimmers and destabilizes downstream swimmers. Animals located far from the conduit's side walls, where the velocity profile is uniform in the plane of motion, are unaffected by these hydrodynamic interactions and do not rheotax. The presence of a stationary wall, a velocity gradient in the plane of motion, and sufficient space for hydrodynamically induced rotation are essential for rheotaxis. The experimental observations were mimicked with great fidelity by computational fluid dynamics simulations, suggesting that hydrodynamic effects are, indeed, the major mechanism involved in rheotaxis.

The effect of proximity to surfaces on rheotaxis behavior explains why some claim that nematodes rheotax (12–19) but others claim that they do not (9–11). Analysis of the literature is complicated by lack of details on the relevant experimental conditions. Lane (9) reported that hookworm larvae did not rheotax when in a glass box but did rheotax when in a capillary tube. This paradox can be interpreted in light of our theory. In the capillary tube, the animals were located close to a surface, whereas in the glass box they were likely far from a surface. Casadevall I Solvas et al. (17) present a video (movie 3) in which *C. elegans* animals situated next to the side wall of a microfluidic device swim upstream whereas animals far from the wall do not.

Can undulatory swimmers exhibit negative rheotaxis (alignment with the flow)? Consider an object moving in an otherwise quiescent liquid. For example, suppose that one of the conduit's walls slides parallel to itself. The head of an animal swimming toward the moving surface will experience higher velocity than its tail. Therefore, this animal will rotate to align with the surface's direction of motion. As before, owing to surface attraction, the animal will remain next to the surface for considerable time intervals with the surface-generated velocity gradient stabilizing the animal's alignment with the flow. Thus, next to moving surfaces we would expect undulatory swimmers to align with the flow (negative rheotaxis).

Rheotaxis has been observed in organisms as simple as single motile cells such as bacteria (7, 29–32) and sperm (6, 33, 34), where hydrodynamics is implicated as the cause of rheotactic behavior (29–34). In contrast, in the case of zebrafish, a vertebrate, an active response of the animal that involves its sensory nervous system is believed to influence the rheotactic behavior (8). Here, through a combination of experiments and numerical simulations, we rule out the possible role of active response of the nematodes in the rheotactic behavior and show that multicellular organisms, such as nematodes, possessing a small nervous system, can exploit passive hydrodynamic mechanisms for directed movement.

Although rheotaxis is involuntary and hydrodynamically induced, it likely plays an important role in nematodes' life cycles. Rheotaxis may assist parasitic nematodes in invading hosts; navigating through veins, arteries, and the lymphatic system; and maintaining their positions in the presence of blood (i.e., the heartworm), lymphatics, or gastric flows. Rheotaxis may assist soil-dwelling nematodes, lacking geotactic behavior (35), to stay near roots and avoid being washed away by rain from regions abundant in food (14). An understanding of the origins of nematode rheotactic behavior could lead to new control and intervention methodologies. For example, drugs suppressing a nematode's motility would reduce the ability of parasitic nematodes to resist flow when residing in humans, animals, and plants to avoid being washed out of the hosts' systems. Understanding of rheotaxis is also important to designers of microfluidic systems for sorting and investigating behaviors of nematodes. Our study suggests the possibility of suppressing the rheotactic behavior by adjusting conduits' dimensions in microfluidic systems.

Materials and Methods

The microfluidic conduit was formed with polydimethylsiloxane using standard soft photolithography. Fluid flow with a constant volumetric flow rate was supplied by a syringe pump (PHD 2000; Harvard Apparatus). Images were

recorded with a digital camera (1600; PCO) through a microscope (20×, BX51; Olympus) and analyzed manually in ImageJ.

Before experiments, animals were cultivated on the surfaces of nematode growth media agar (36), fed with bacteria DA837 (37), and kept at a constant temperature of 20 °C in an incubator. The wild-type strain N2, variety Bristol was used (36). All of the experiments were carried out with well-fed hermaphrodites, 1 d after the fourth larval stage, during early adulthood. Large numbers of same-age animals were obtained using the alkaline bleach method (38).

ACKNOWLEDGMENTS. We thank Professors J. B. Lok and R. M. Greenberg (School of Veterinary Medicine, University of Pennsylvania) for information on parasitic nematodes. This research was supported, in part, by NIH National Institute on Aging Grant 5R03AG042690-02 and by National Science Foundation Nanoscale Science and Engineering Center Grant DMR08-32802 to the University of Pennsylvania. D.M.R. was supported by NIH Grant R01NS064030. Strains of *C. elegans* used in this study were obtained from the Caenorhabditis Genetics Center, which is funded by the NIH Office of Research Infrastructure Programs (P40 OD010440).

1. Chen ZX, Chen SY, Dickson DW (2004) *Nematology: Advances and Perspectives* (CABI, Wallingford, UK), Vol 1.
2. Chen ZX, Chen SY, Dickson DW (2004) *Nematology: Advances and Perspectives* (CABI, Wallingford, UK), Vol 2.
3. Albonico M, et al. (2008) Controlling soil-transmitted helminthiasis in pre-school-age children through preventive chemotherapy. *PLoS Negl Trop Dis* 2(3):e126.
4. May RM (2007) Parasites, people and policy: Infectious diseases and the Millennium Development Goals. *Trends Ecol Evol* 22(10):497–503.
5. Gaugler R, Bilgrami AL (2004) *Nematode Behaviour* (CABI, Wallingford, UK).
6. Bretherton FP, Rothschild L (1961) Rheotaxis of spermatozoa. *Proc R Soc Lond B Biol Sci* 153(953):490–502.
7. Rosengarten R, Klein-Struckmeier A, Kirchhoff H (1988) Rheotactic behavior of a gliding mycoplasma. *J Bacteriol* 170(2):989–990.
8. Suli A, Watson GM, Rubel EW, Raible DW (2012) Rheotaxis in larval zebrafish is mediated by lateral line mechanosensory hair cells. *PLoS ONE* 7(2):e29727.
9. Lane C (1930) Behaviour of infective hookworm larvae. *Ann Trop Med Parasitol* 24(3): 411–421.
10. Wallace HR (1961) The orientation of *Ditylenchus dipsaci* to physical stimuli. *Nematologica* 6(3):222–236.
11. Wallace HR (1959) Movement of eelworms. V. Observations on Aphelenchoides ritzema-bosi (Schwartz, 1912) Steiner, 1932 on florists' chrysanthemums. *Ann Appl Biol* 47(2):350–360.
12. Adamo JA, Madamba CP, Chen TA (1976) Vertical migration of the rice white-tip nematode, Aphelenchoides besseyi. *J Nematol* 8(2):146–152.
13. Pinkerton JN, Mojtahedi H, Santo GS, O'Bannon JH (1987) Vertical migration of Meloidogyne chitwoodi and M. hapla under controlled temperature. *J Nematol* 19(2): 152–157.
14. Fujimoto T, Hasegawa S, Otobe K, Mizukubo T (2010) The effect of soil water flow and soil properties on the mobility of second-stage juveniles of the root-knot nematode (Meloidogyne incognita). *Soil Biol Biochem* 42(7):1065–1072.
15. Fujimoto T, Hasegawa S, Otobe K, Mizukubo T (2009) Effect of water flow on the mobility of the root-knot nematode Meloidogyne incognita in columns filled with glass beads, sand or andisol. *Appl Soil Ecol* 43(2-3):200–205.
16. Chabrier C, Carles C, Quénéhervé P, Cabidoche Y-M (2008) Nematode dissemination by water leached in soil: Case study of Radopholus similis (Cobb) Throne on nitisol under simulated rainfall. *Appl Soil Ecol* 40(2):299–308.
17. Casadevall i Solvas X, et al. (2011) High-throughput age synchronisation of Caenorhabditis elegans. *Chem Commun (Camb)* 47(35):9801–9803.
18. Albrecht DR, Bargmann CI (2011) High-content behavioral analysis of Caenorhabditis elegans in precise spatiotemporal chemical environments. *Nat Methods* 8(7):599–605.
19. Wallace HR (1963) *The Biology of Plant Parasitic Nematodes* (Edward Arnold, London).
20. Yuan J, Raizen DM, Bau HH (2014) Why are undulatory swimmers attracted to surfaces (bordertaxis)? *67th Annual Meeting of the American Physical Society Division of Fluid Dynamics*. Available at gfm.aps.org/meetings/dfd-2014/54174d3369702d585c040300. Accessed February 26, 2015.
21. Yuan J, Raizen DM, Bau HH (2014) Gait synchronization in Caenorhabditis elegans. *Proc Natl Acad Sci USA* 111(19):6865–6870.
22. Pierce-Shimomura JT, Morse TM, Lockery SR (1999) The fundamental role of pirouettes in Caenorhabditis elegans chemotaxis. *J Neurosci* 19(21):9557–9569.
23. Schulman RD, Backholm M, Ryu WS, Dalnoki-Veress K (2014) Undulatory microwimming near solid boundaries. *Phys Fluids* 26(10):101902.
24. Gray J, Lissmann HW (1964) The locomotion of nematodes. *J Exp Biol* 41(1):135–154.
25. Sznitman J, Shen X, Sznitman R, Arratia PE (2010) Propulsive force measurements and flow behavior of undulatory swimmers at low Reynolds number. *Phys Fluids* 22(12):121901.
26. Bargmann CI (2006) Chemosensation in *C. elegans*. *WormBook*, ed The *C. elegans* Research Community, 10.1895/wormbook.1.123.1. Available at www.wormbook.org.
27. Ryu WS, Samuel ADT (2002) Thermotaxis in Caenorhabditis elegans analyzed by measuring responses to defined Thermal stimuli. *J Neurosci* 22(13):5727–5733.
28. Gabel CV, et al. (2007) Neural circuits mediate electrosensory behavior in Caenorhabditis elegans. *J Neurosci* 27(28):7586–7596.
29. Hill J, Kalkanci O, McMurry JL, Koser H (2007) Hydrodynamic surface interactions enable Escherichia coli to seek efficient routes to swim upstream. *Phys Rev Lett* 98(6):068101.
30. Kaya T, Koser H (2012) Direct upstream motility in Escherichia coli. *Biophys J* 102(7): 1514–1523.
31. Shen Y, Siryaporn A, Lecuyer S, Gitai Z, Stone HA (2012) Flow directs surface-attached bacteria to twitch upstream. *Biophys J* 103(1):146–151.
32. Marcos, Fu HC, Powers TR, Stocker R (2012) Bacterial rheotaxis. *Proc Natl Acad Sci USA* 109(13):4780–4785.
33. Miki K, Clapham DE (2013) Rheotaxis guides mammalian sperm. *Curr Biol* 23(6): 443–452.
34. Kantsler V, Dunkel J, Blayney M, Goldstein RE (2014) Rheotaxis facilitates upstream navigation of mammalian sperm cells. *eLife* 3:e02403.
35. Eo J, Otobe K, Mizukubo T (2008) Absence of geotaxis in soil-dwelling nematodes. *Nematology* 10(1):147–149.
36. Brenner S (1974) The genetics of *Caenorhabditis elegans*. *Genetics* 77(1):71–94.
37. Davis MW, et al. (1995) Mutations in the *Caenorhabditis elegans* Na,K-ATPase α-subunit gene, *eat-6*, disrupt excitable cell function. *J Neurosci* 15(12):8408–8418.
38. Stiernagle T (2006) Maintenance of *C. elegans*. *WormBook*, ed The *C. elegans* Research Community, 10.1895/wormbook.1.101.1. Available at www.wormbook.org.